OPEN ACCESS

Original research

Serum lipidome unravels a diagnostic potential in bile acid diarrhoea

Monika Lewinska ,[1] Martin Lund Kårhus,[2] Anne-Marie Gade Ellegaard ,[2] Manuel Romero-Gómez ,[3] Rocio I R Macias ,[4] Jesper B Andersen ,[1] Filip Krag Knop [2,5,6]

► Additional supplemental material is published online only. To view, please visit the journal online (http://dx.doi.org/10.1136/gutjnl-2022-329213).

For numbered affiliations see end of article.

Correspondence to
Professor Filip Krag Knop, Center for Clinical Metabolic Research, Copenhagen University Hopital - Herlev and Gentofte, Hellerup, DK-2900, Denmark;
filip.krag.knop.01@regionh.dk
Dr Jesper B Andersen;
jesper.andersen@bric.ku.dk

ML and MLK contributed equally.
JBA and FKK contributed equally.

Received 29 November 2022
Accepted 30 March 2023

ABSTRACT

Objective Bile acid diarrhoea (BAD) is debilitating yet treatable, but it remains underdiagnosed due to challenging diagnostics. We developed a blood test-based method to guide BAD diagnosis.

Design We included serum from 50 treatment-naive patients with BAD diagnosed by gold standard ^{75}selenium homotaurocholic acid test, 56 feature-matched controls and 37 patients with non-alcoholic fatty liver disease (NAFLD). Metabolomes were generated using mass spectrometry covering 1295 metabolites and compared between groups. Machine learning was used to develop a BAD Diagnostic Score (BDS).

Results Metabolomes of patients with BAD significantly differed from controls and NAFLD. We detected 70 metabolites with a discriminatory performance in the discovery set with an area under receiver-operating curve metric above 0.80. Logistic regression modelling using concentrations of decanoylcarnitine, cholesterol ester (22:5), eicosatrienoic acid, L-alpha-lysophosphatidylinositol (18:0) and phosphatidylethanolamine (O-16:0/18:1) distinguished BAD from controls with a sensitivity of 0.78 (95% CI 0.64 to 0.89) and a specificity of 0.93 (95% CI 0.83 to 0.98). The model was independent of covariates (age, sex, body mass index) and distinguished BAD from NAFLD irrespective of fibrosis stage. BDS outperformed other blood test-based tests (7-alpha-hydroxy-4-cholesten-3-one and fibroblast growth factor 19) currently under development.

Conclusions BDS derived from serum metabolites in a single-blood sample showed robust identification of patients with BAD with superior specificity and sensitivity compared with current blood test-based diagnostics.

WHAT IS ALREADY KNOWN ON THIS TOPIC

⇒ Bile acid diarrhoea (BAD) is a common disorder estimated to affect 1% of the population worldwide though many patients remain undiagnosed. The current gold standard for BAD diagnosis is ^{75}selenium homotaurocholic acid test, which is not approved in several countries (including USA). The fibroblast growth factor 19 and 7-alpha-hydroxy-4-cholesten-3-one currently aid BAD diagnosis, but their accuracy is low. The BAD metabolic landscape is unknown.

WHAT THIS STUDY ADDS

⇒ This is the first study presenting a comprehensive serum lipidomic and metabolomic landscape of patients with BAD at the time of diagnosis. Significant alterations in metabolomic profiles allowed the development of a serum-based diagnostic model and prediction of treatment response.

HOW THIS STUDY MIGHT AFFECT RESEARCH, PRACTICE OR POLICY

⇒ The new diagnostic model based on a single serum sample may improve and accelerate the diagnostic process and, thus, increase treatment accessibility. Also, the serum-based prediction of treatment response may spur improved individualisation of BAD treatment.

INTRODUCTION

Bile acid diarrhoea (BAD) is a gastrointestinal disease with high stool frequency, diarrhoea, faecal urgency and incontinence as primary symptoms.[1] It is caused by a pathophysiological spill-over of bile acids to the colon, where these natural detergent molecules irritate the colonic mucosa causing the abovementioned symptoms.[1–3] BAD can be idiopathic (primary BAD) or secondary to other diseases such as inflammatory bowel disease, coeliac disease or cholecystectomy.[1 4–12] Due to the nature of the symptoms, BAD is a socially debilitating disease with a high cost to the individual[13] and at the societal level.[14 15] BAD is normally treated with bile acid sequestrants that bind bile acids in the intestinal lumen diminishing the symptoms, but the effect of bile acid sequestrants is variable and they are associated with gastrointestinal side effects.[16–18] Recently, a new treatment strategy based on the glucagon-like peptide 1 (GLP-1) receptor agonist liraglutide has shown promising results.[19] Studies have estimated that the prevalence of BAD is 1% in the adult population,[9 20–22] but BAD is heavily underdiagnosed partly due to the use of different and often challenging diagnostic procedures. BAD can be diagnosed in several ways, but currently, the most accurate diagnostic test is the ^{75}selenium homotaurocholic acid (SeHCAT) test where the 7-day retention of an orally administered radiolabelled bile acid is measured.[23] The SeHCAT test

To cite: Lewinska M, Kårhus ML, Ellegaard A-MG, *et al*. *Gut* Epub ahead of print: [*please include* Day Month Year]. doi:10.1136/gutjnl-2022-329213

is not approved in all countries (including USA) where instead a 48-hour stool collection,[24] trial and error with bile acid sequestrants[17 18] or a breath test[16 25 26] can be used. Also, 7-alpha-hydroxy-4-cholesten-3-one (C4),[24 27] which represents a surrogate marker for bile acid synthesis, and fibroblast growth factor 19 (FGF19), a surrogate marker of bile acid resorption and regulator of bile acid metabolism, can be used to diagnose BAD. All the current diagnostic methods have limitations. The SeHCAT test is expensive, entails radioactive exposure and requires two visits to the clinic with precisely 7 days interval; 48-hour stool collection is time-consuming and irksome; trial and error with bile acid sequestrants has a potential high false-negative rate; and the breath test is imprecise and time-consuming.[24] Using C4 or FGF19 as diagnostic tools have still not been standardised for clinical use and often presents low sensitivity.[28–30] Thus, new accurate diagnostic tools, which can be used worldwide, at low cost and with minimal intervention, are urgently needed.

Here, we investigated the untargeted metabolomic and lipidomic serum landscapes of primary BAD and used machine learning to take an unbiased approach to the development of a blood test-based diagnostic tool.

MATERIALS AND METHODS

Patients

Serum samples were collected from fasting, treatment-naive patients at the time of diagnosis (SeHCAT method) at Gentofte Hospital, University of Copenhagen, under the clinical protocol number EudraCT 2018-003575-34.[19]. Written informed consent was obtained from all participants. The study was approved in accordance with institutional review board approval number 504-0307/22-5000. Patients with non-alcoholic fatty liver disease (NAFLD) (n=37) and controls (CTRLs) included in this study were previously described.[5 31] Out of 37 patients with NAFLD, 17 showed simple steatosis with no/limited fibrosis and 20 patients had non-alcoholic steatohepatitis (NASH). Clinical characteristics of BAD, patients with NAFLD and CTRLs are presented in table 1. Neither patients nor the public was involved in designing or evaluating the study.

Metabolite extraction and profiling

In brief, metabolites were measured in serum using four platforms (lipidomic platforms 1 and 2, amino acid platform 3 and oxylipins) at One Way Liver, S.L. The approach combines the ultra high-performance liquid chromatography and mass spectrometry approaches were used allowing extensive profiling of circulating metabolome. A detailed description of metabolomic profiling is in online supplemental material and methods.

Table 1 Clinical characteristics of study population

	CTRL n=56	BAD n=50	NAFLD=37	P value
Sex				
Female %	58	64	65	0.76
Male %	42	36	35	
Age	50.2±14.5	50.2±12.9	50.5±11.5	0.99
Body mass index (kg/m^2)	29.0±7.0	29.9±5.0	42.7±8.7	**<0.0001***†
Alanine transaminase (U/L)	28.0±13.2	33.2±16.0	27.2±10.7	0.11
Alkaline phosphatase (U/L)	72.7±30.8	78.3±17.9	69.8±18.5	0.32
Bilirubin (mg/dL)	0.66±0.30	0.57±0.19	0.51±0.24	0.10

The values are expressed by mean±SD. P values arise from one-way analysis of variance or Fisher's exact test.
*NAFLD versus BAD.
†NAFLD versus CTRL.

Statistical analysis

The detailed statistical analyses are presented in online supplemental material and methods. In short, differences in biochemical parameters were established using Mann-Whitney for non-normally distributed values, t-test for normally distributed values and Fisher"s exact test for categorical data (Prism V.9.3.0, GraphPad software, USA). The covariate-testing and correction were performed with linear regression before analysis. Covariates included age, sex and body mass index (BMI), as well as batch, which were adjusted in differential expression analysis (R V.4.0.4, R Core Team (2022)). Receiver operating characteristic (ROC) curve analysis was used to identify and evaluate the performance of individual metabolites (MetaboAnalyst V.5.0).[32] The post hoc power analysis established the minimal sample size of 24 samples per group at false discovery rate corrected p value=0.05, and statistical power of 90%. The linear support vector machine (SVM) method was used for sample classification. Feature selection was performed with SVM mean importance measure. A logistic regression model was generated to calculate the BAD Diagnostic Score (BDS). Metabolite selection was performed based on the SVM mean importance measure and LASSO Frequencies (MetaboAnalyst V.5.0),[32] which were used to generate the logistic regression equation: $\mathbf{logit(P) = ln(P / (1 - P)) = \alpha + \beta X}$, where α is the intercept term, β is the regression coefficient estimated from the sample data set, X_i is the set of covariate (concentration) values, and $P=Pr(y=1|x)$ is the probability of the disease (ie, BAD).

RESULTS

Enrolment and metabolic characterisation of patients

Serum samples obtained from 50 patients with SeHCAT-verified primary BAD were subjected to untargeted metabolomics using ultra-high performance liquid chromatography-mass spectrometry (UHPLC-MS). In total, we detected 427 metabolites including amino acids, bile acids, fatty acids, glycerolipids and steroids (online supplemental figure 1A). Fifteen patients within the BAD cohort had previously undergone a cholecystectomy, but we observed no difference in their serum metabolomic profiles compared with the remaining 35 patients with BAD (online supplemental figure 2A,B). In terms of age, sex, BMI and normal liver function, based on biochemical measures such as alanine transaminase (ALT) and alkaline phosphatase, we found no difference between patients with BAD and CTRLs (table 1). Furthermore, we compared patients with BAD to 37 patients with age-matched and sex-matched NAFLD (17 with simple steatosis and 20 with NASH). Patients with NAFLD had significantly higher BMI compared with CTRL and patients with BAD, but retained normal liver function based on ALT, alkaline phosphatase and bilirubin (table 1).

Development of the BDS

To develop a serum-based diagnostic model for BAD, we randomised all samples into two sets: a discovery (DISCO) set, comprising 25 patients with BAD and 25 feature-matched CTRLs, and a validation (VALID) set, consisting of the remaining 25 patients with BAD and 31 feature-matched CTRLs. First, we computed the area under ROC (AUROC) univariate analysis for all 427 significantly detected metabolites and found that 70 metabolites presented a promising diagnostic potential with a discriminatory performance metric above 0.80 and p

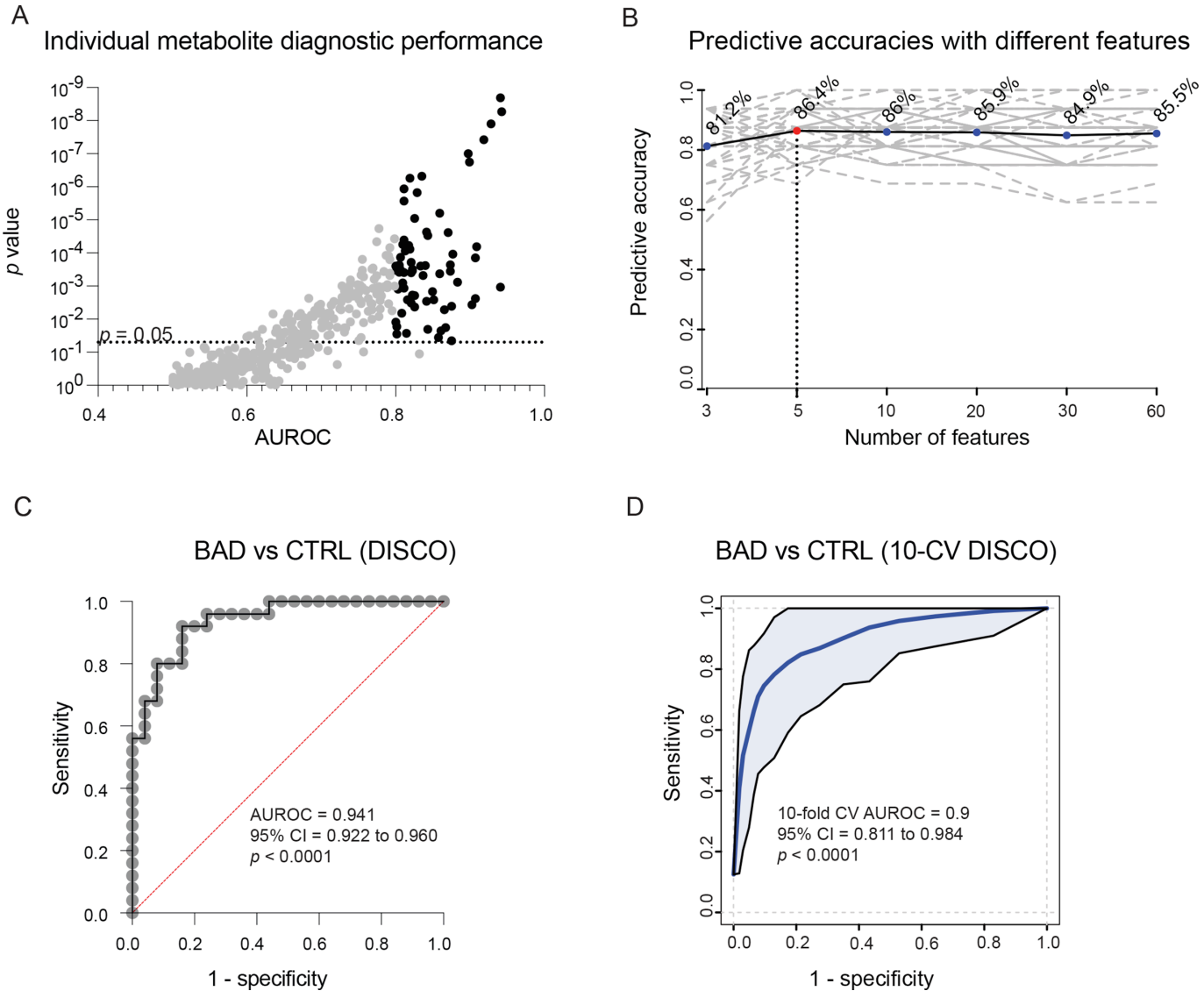

Figure 1 Diagnostic potential of serum metabolites. (A) The area under receiver operating characteristic (AUROC) curve and p values of individual metabolites distinguishing bile acid diarrhoea (BAD) from controls (CTRLs) in the discovery set. The dotted line indicates a p value of 0.05. Black dots represent metabolites with AUROC >0.8 and p<0.05. (B) The predictive accuracies of support vector machine models with different numbers of features. (C) The receiver operating characteristic curve (ROC) of BAD Diagnostic Score in the discovery set. (D) 10-cross validation (10-CV) of BAD Diagnostic score (BDS) in the discovery (DISCO) set showing 95% CI band in shaded area.

value <0.05 (figure 1A, online supplemental figure 1B, online supplemental table 1). Next, we used the linear SVM algorithm to determine if a specific combination of metabolites would improve the diagnostic potential of individual metabolites. We established that the best performance was a combination of five metabolites with an 86% accuracy or above (figure 1B). As such, we employed logistic regression using metabolites with the highest mean importance measures to complete the diagnostic model. From this step, we generated the BDS, which is based on logistic regression modelling including the five metabolites. The BDS is calculated as: *logit(P) = log(P / (1 − P)) = −2.362 to 1.09 × decanoylcarnitine − 1.007 × cholesterol ester (22:5) + 1.229 × phosphatidylethanolamine (O-16:0/18:1) + 2.227 × L-alpha-lysophosphatidylinositol (18:0) + 6.344 × eicosatrienoic acid* with a cut-off value of 0.59.

The diagnostic potential of the BDS achieved an AUROC of 0.94 with a sensitivity of 0.83 (95% CI 0.78 to 0.88) and specificity of 0.89 (95% CI 0.85 to 0.93) (figure 1C). To test our model, we used the 10-fold cross-validation resampling method that reached an AUROC of 0.90 (95% CI 0.81 to 0.98), sensitivity of 0.84 (95% CI 0.84 to 0.98) and specificity of 0.84 (95% CI 0.70 to 0.98) (figure 1D).

Validation of the BDS

To validate the model in an independent sample set, we calculated BDS in the additional 25 patients with BAD (VALID) and compared with the remaining 31 feature-matched CTRLs. BDS significantly distinguished patients with BAD from CTRLs in the validation set with an AUROC of 0.91 (95% CI 0.83 to 0.99), sensitivity of 0.74 (95% CI 0.57 to 0.86) and specificity of 0.84 (95% CI 0.65 to 0.94) (figure 2A). Furthermore, combining the DISCO and VALID data sets the BDS had a sensitivity of 0.78 (95% CI 0.64 to 0.89) and a specificity of 0.93 (95% CI 0.83 to 0.98). The relative abundance of BDS metabolites in BAD (DISCO), BAD (VALID) and NAFLD are presented in figure 2C.

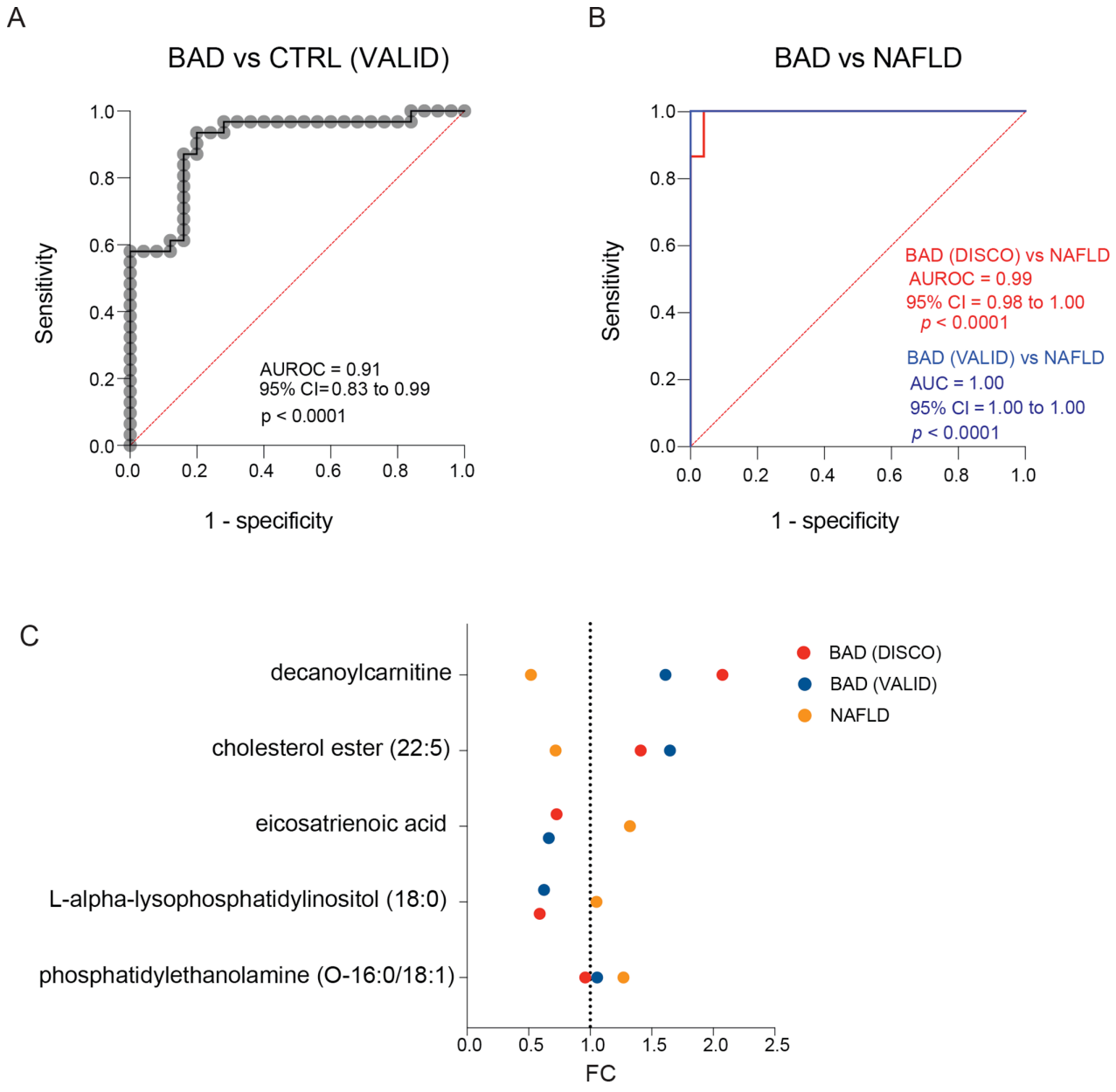

Figure 2 Validation of BAD Diagnostic Score. (A) The receiver operating characteristic (ROC) curve of bile acid diarrhoea (BAD) Diagnostic Score in the validation (VALID) set. (B) ROC curve of BAD Diagnostic Score of BAD discovery (DISCO) and validation sets against non-alcoholic fatty liver disease (NAFLD) patients. (C) Waterfall plot presenting the relative abundance of BDS metabolites in relation to control (CTRL) in BAD (DISCO), BAD (VALID) and patients with NAFLD groups. FC, fold change.

Multivariate analysis showed that BDS is independent of the covariates age, sex, and BMI (p=0.54, p=0.20, and p=0.22, respectively). Since BAD has been shown to share similarities with NAFLD, with altered regulation of fibroblast growth factor receptor 4/FGF19 and Klotho beta pathways, we next compared BDS to a serum data set of 37 patients with NAFLD. In comparison to NAFLD, both BAD DISCO and VALID sets were significantly different (figure 2B), and BDS was independent of the liver fibrosis score (online supplemental figure 3A–C). Importantly, the diagnostic yield (defined as the proportion of patients with true positive BAD) for the BDS reached 90%, while FGF19 (cut-off <145 pg/mL) reached 70% and C4 (cut-off >48.7 ng/mL) reached only 56%, both significantly inferior to BDS. Furthermore, combining FGF19 and C4 (reaching cut-off of either FGF19 or C4) improved diagnostic yield to 82% remaining inferior to BDS.

Serum metabolomic landscape of BAD

To investigate the metabolomic landscapes of patients with BAD, we merged the cohorts (DISCO and VALID sets) and performed a pair-wise comparison of patients with BAD (n=50) and CTRLs (n=56). We first examined the concentration of bile acids in the systemic circulation (figure 3). As such, we found that patients with BAD presented significantly higher (p=0.035) concentrations of primary bile acids (cholic acid and chenodeoxycholic acid combined) (figure 3B), with an increased abundance specifically of unconjugated and glycine-conjugated bile acid species (p=0.0006 and p=0.0075, respectively) (figure 3D and F). On the contrary, secondary bile acids (figure 3C and H–K) and primary taurine-conjugated bile acids (figure 3G) remained unchanged between patients with BAD and matched CTRLs. Notably, serum bile acid levels of patients with NAFLD did not

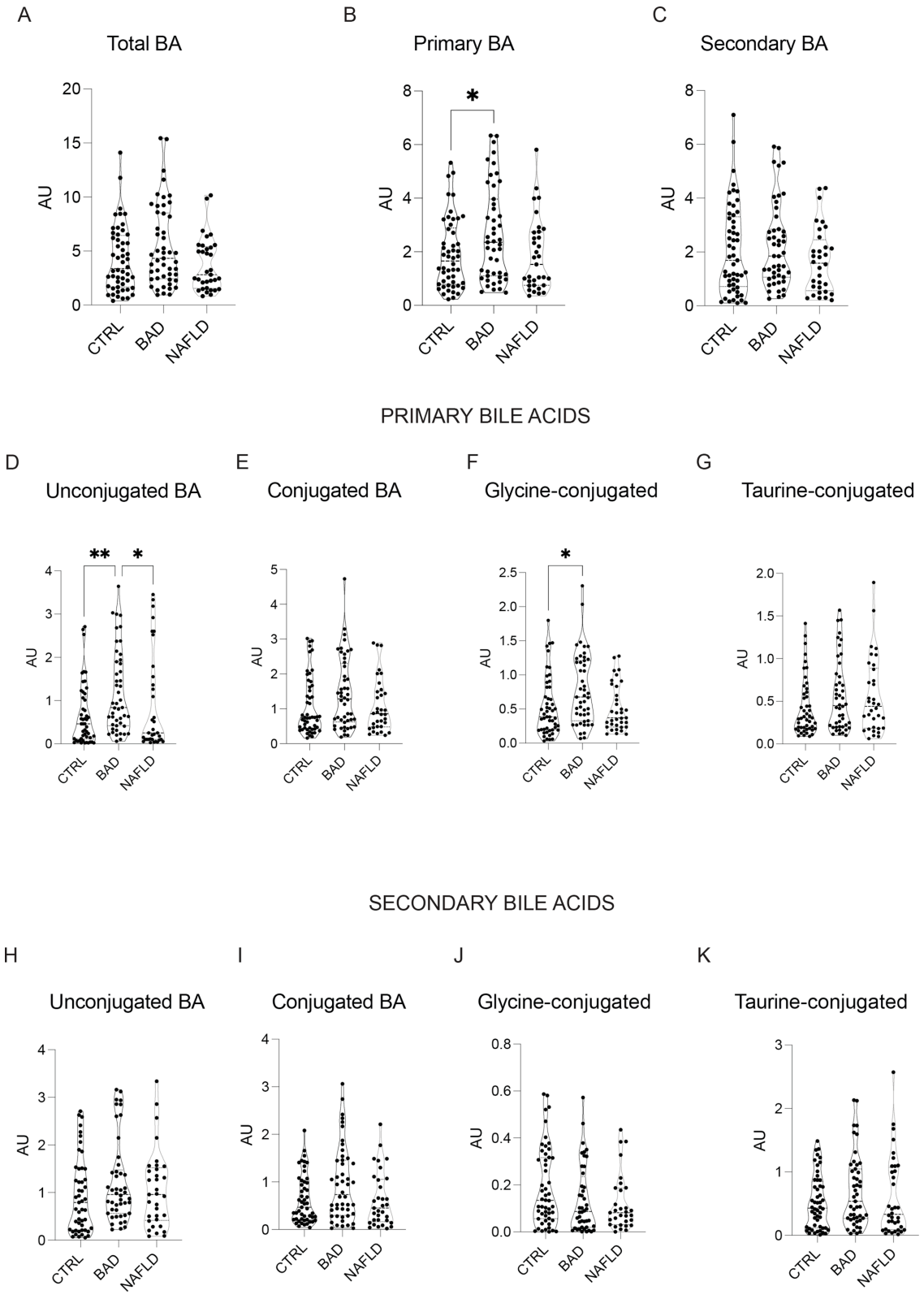

Figure 3 Serum bile acid concentrations in patients with BAD. (A) The abundance of total bile acids (BA) in serum of bile acid diarrhoea (BAD) patients, controls (CTRLs) and patients with non-alcoholic fatty acid liver disease (NAFLD). (B) The abundance of primary BA in serum of BAD, CTRL and NAFLD. (C) The abundance of secondary BA in serum of BAD, CTRL and NAFLD. (D) The abundance of primary unconjugated BA in serum of BAD, CTRL and NAFLD. (E) The abundance of primary conjugated BA in serum of BAD, CTRL and NAFLD. (F) The abundance of primary glycine-conjugated BA in serum of BAD, CTRL and NAFLD. (G) The abundance of primary taurine-conjugated BA in serum of BAD, CTRL and NAFLD. (H) The abundance of secondary unconjugated BA in serum of BAD, CTRL and NAFLD. (I) The abundance of secondary conjugated BA in serum of BAD, CTRL and NAFLD. (J) The abundance of secondary glycine-conjugated BA in serum of BAD, CTRL and NAFLD. (K) The abundance of primary taurine-conjugated BA in serum of BAD, CTRL and NAFLD, *p<0.05, **p<0.01, ***p<0.0001, ****p<0.00001, Mann-Whitney test. AU, arbitrary unit; ns, not statistically significant.

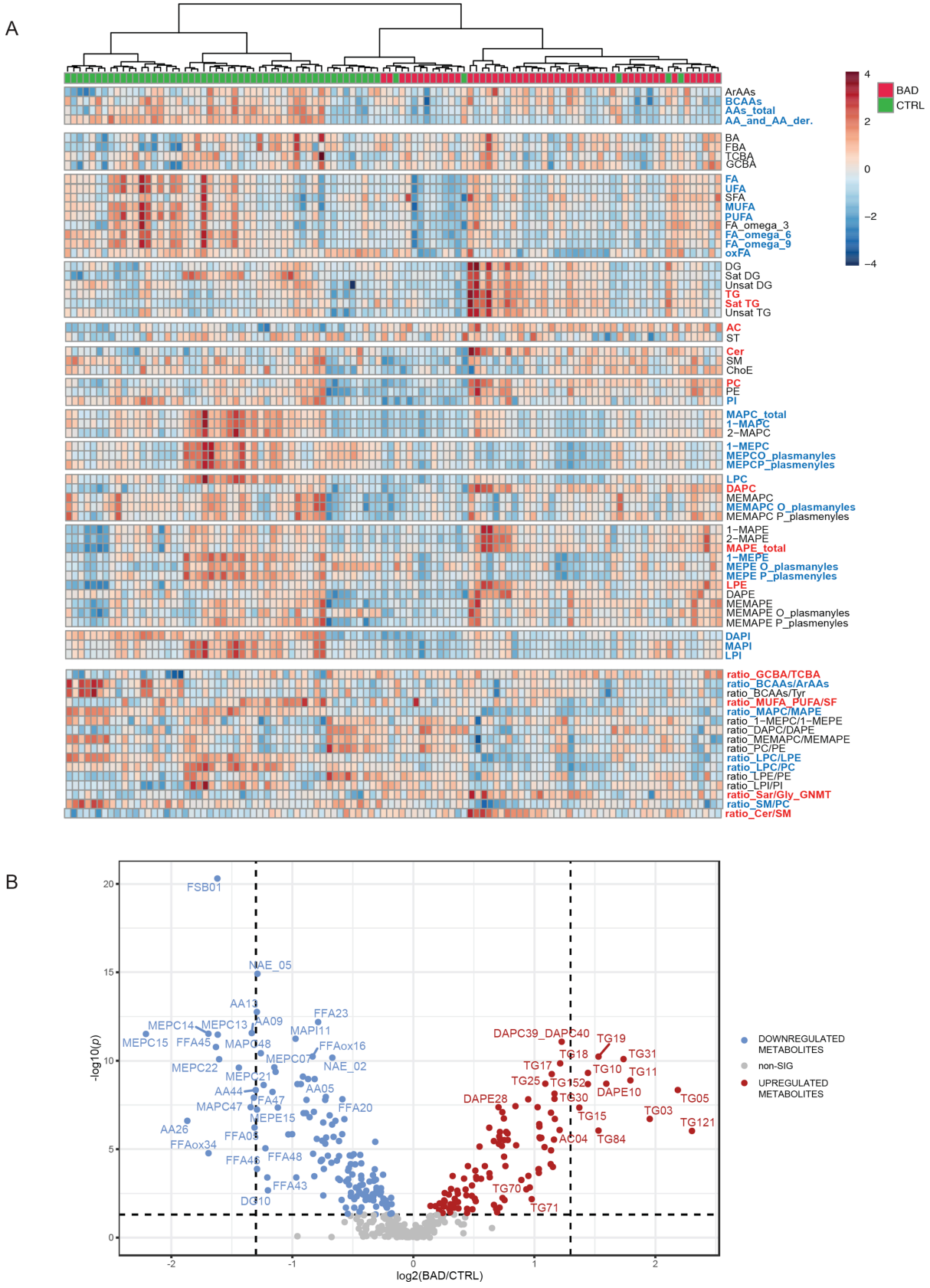

Figure 4 Serum metabolomic landscape of patients with BAD. (A) Heatmap representing classes of metabolites and rations of metabolic classes. Significantly different (t-test, p<0.05) classes of metabolites are bold, blue colour indicates depleted and red upregulated metabolic classes in patients with BAD. (B) Volcano plot presenting differentially abundant (false discovery rate corrected p<0.05) metabolites between patients with bile acid diarrhoea (BAD) and controls (CTRL). Each dot represents one metabolite; grey colour indicates no significant difference (non-SIG), blue colour indicates significantly downregulation in patients with BAD and red colour indicates significantly upregulation in patients with BAD. For abbreviations, see online supplemental table 10.

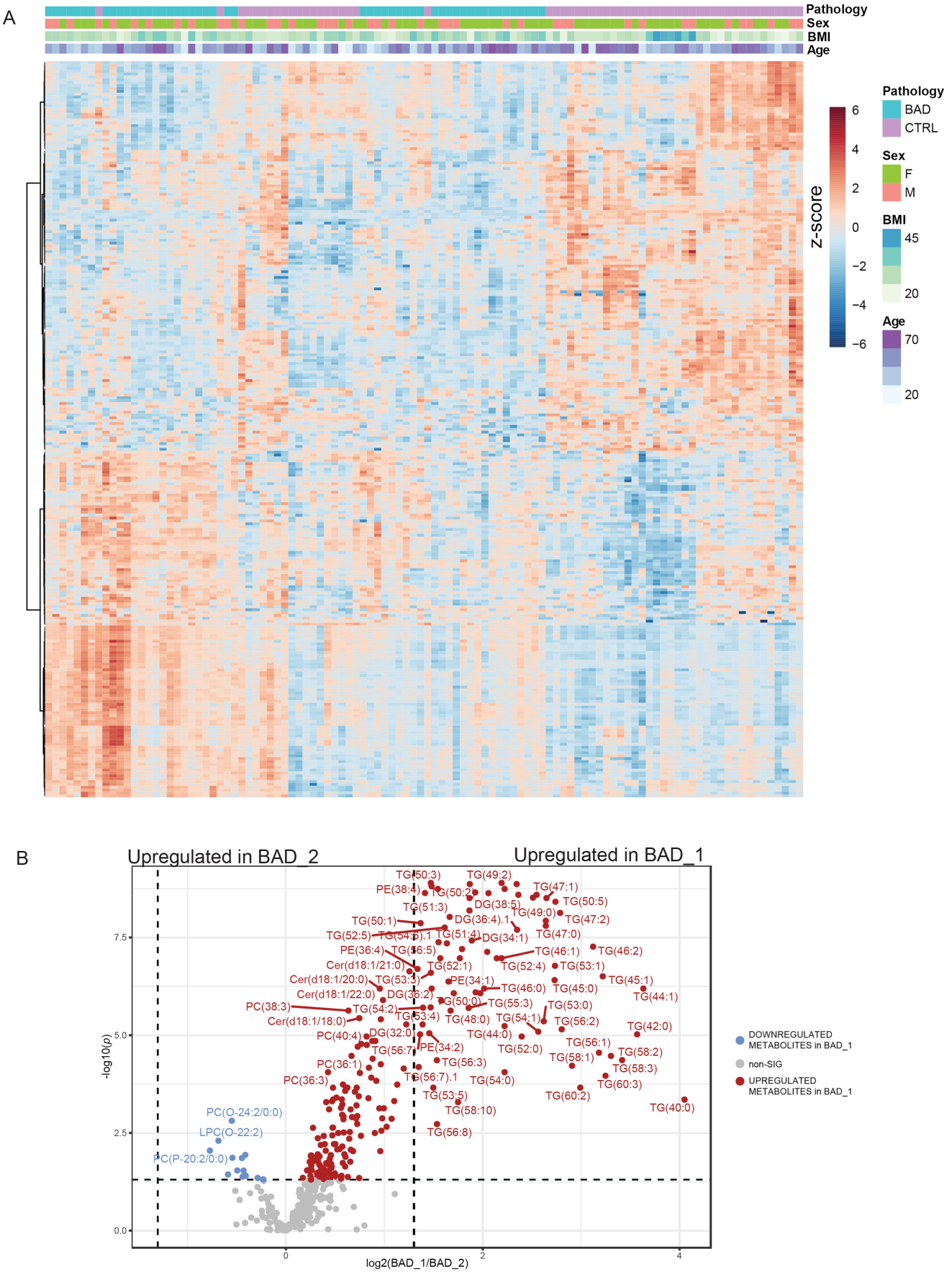

Figure 5 Serum metabolomics identifies two distinctive clusters of patients with bile acid diarrhoea (BAD). (A) Heatmap representing unsupervised hierarchical clustering of BAD and controls (CTRL) identifying two clusters of patients with BAD. (B) Volcano plot representing differentially abundant metabolites between two BAD clusters. BMI, body mass index.

Table 2 Clinical characteristics of BAD clusters

	BAD_1 n=25	BAD_2 n=25	P value
Sex			
Female %	44	28	0.38
Male %	56	72	
Age	53.6±11.3	46.8±13.5	0.06
Body mass index (kg/m^2)	31.9±4.5	27.9±4.8	**0.004**
Alanine transaminase (U/L)	39.7±16.0	26.5±12.9	**0.003**
Alkaline phosphatase (U/L)	81.8±20.9	74.6±13.0	0.16
Bilirubin (mg/dL)	0.58±0.20	0.56±0.17	0.83
FGF19 (pg/ml)	109.3±85.22	101.0±77.88	0.66
Triglycerides (mmol/l)	2.1±1.0	2.6±2.4	0.89
SeHCAT (%)	3.53±2.96	4.13±3.50	0.52
Stools/day (baseline)	3.82±1.89	3.25±1.77	0.28

The values are expressed by mean±SD. P values arise from paired t-tests or Mann-Whitney test.
Statistically significant P values are marked with bold font.
BAD, bile acid diarrhoea; FGF19, fibroblast growth factor 19; SeHCAT, ^{75}selenium homotaurocholic acid test.

differ from CTRLs (figure 3). Next, we sought to investigate the differences in the metabolic classes. Among a total of 72 metabolic classes, and the ratios of these metabolites, 42 metabolic classes showed significant deregulation in the metabolomes of patients with BAD (false discovery rate-adjusted p<0.05). The serum of patients with BAD was significantly depleted in amino acids, fatty acids and glycerophospholipids, whereas acylcarnitines, triglycerides (TGs), ceramides, phosphatidylcholines, phosphatidylethanolamines, and lysophosphatidylethanolamines showed increased concentrations. Moreover, we observed a significantly higher sarcosine/glycine ratio in patients with BAD, which may suggest an increased glycine N-methyltransferase activity causing the breakdown of methionine (figure 4A, online supplemental table 2).

Differential abundance analysis on individual metabolites was performed using a linear model adjusting for covariates (age, sex and BMI) and batch correction. We detected 256 significantly different metabolites, of which 119 were significantly upregulated and 137 were depleted in the serum of patients with BAD (figure 4B, online supplemental table 3). In patients with BAD, the most abundant metabolites were TGs, while monoetherglycerophosphocholines and free fatty acids were significantly depleted compared with the level of these metabolites in CTRLs. Thus, we quantified the levels of oxylipins in 50 patients with BAD (compared with a random subset of the CTRLs, n=12), showing that oxylipins like free fatty acids were significantly depleted in patients with BAD, with the only exception of an increase in the unsaturated fatty acid 14,15-DiHETE (online supplemental table 4). Using BioPAN[33] to perform lipid pathway enrichment analysis, we identified an increased activity of choline phosphotransferase 1, sphingomyelin phosphodiesterase 1 and 4 and fatty acid desaturases (online supplemental figure 4). Interestingly, the unsupervised hierarchical clustering of all metabolites revealed two distinct BAD clusters (figure 5A), with a significant difference in the level of TG species (figure 5B), which was not detected by routine blood testing (table 2). Cluster 1 (BAD_1) represented patients with a significantly higher BMI (t-test, p=0.004) and elevated ALT levels (t-test, p=0.003) compared

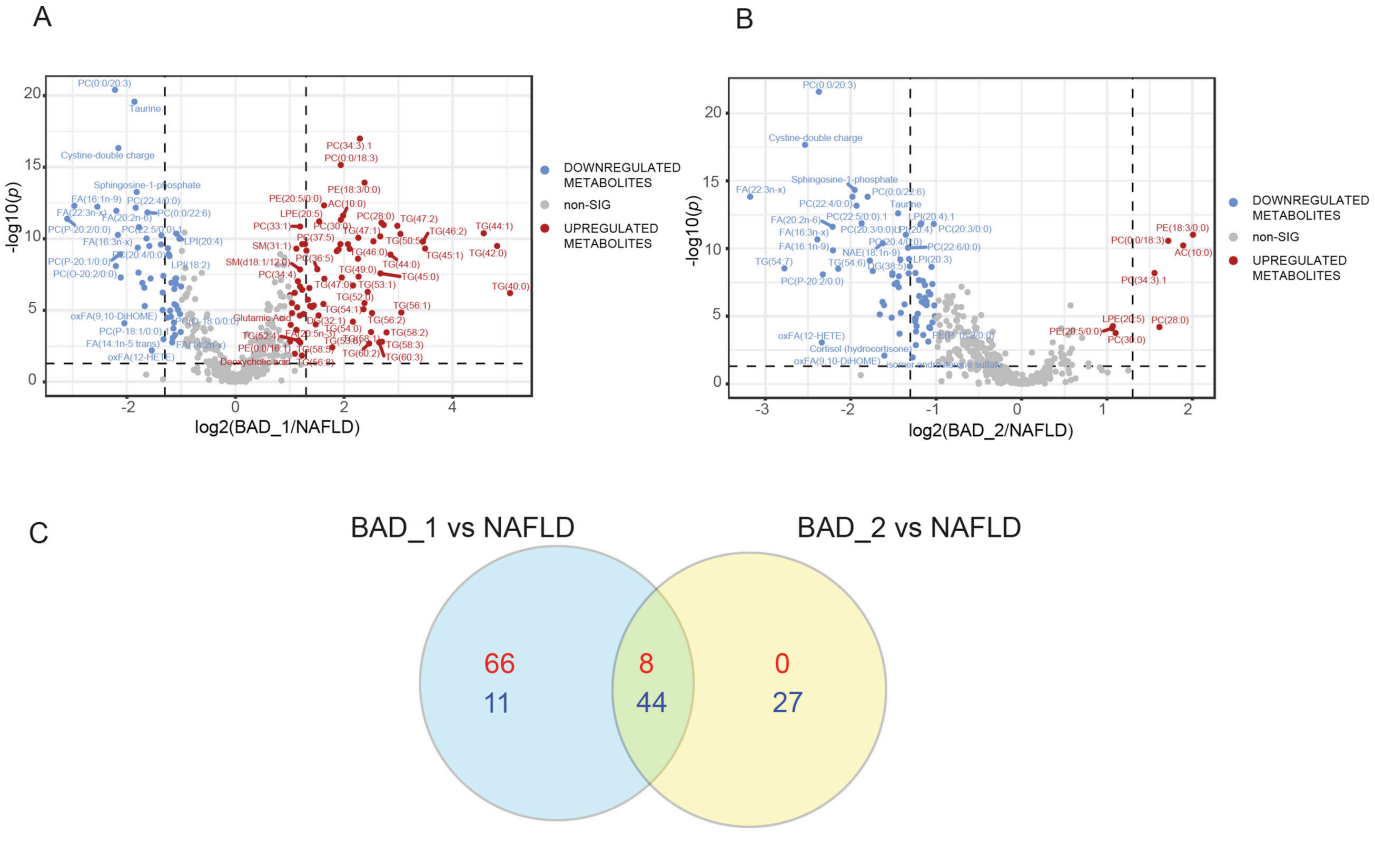

Figure 6 Differential metabolomic profiles of two bile acid diarrhoea BAD clusters. (A) Volcano plot illustrating differentially expressed metabolites (DEM) between BAD_1 cluster and patients with non-alcoholic fatty liver disease (NAFLD). (B) Volcano plot illustrating DEM between BAD_2 cluster and patients with NAFLD. (C). Venn diagram representing DEM (upregulated (red) and reduced (blue)) in patients with BAD compared with NAFLD.

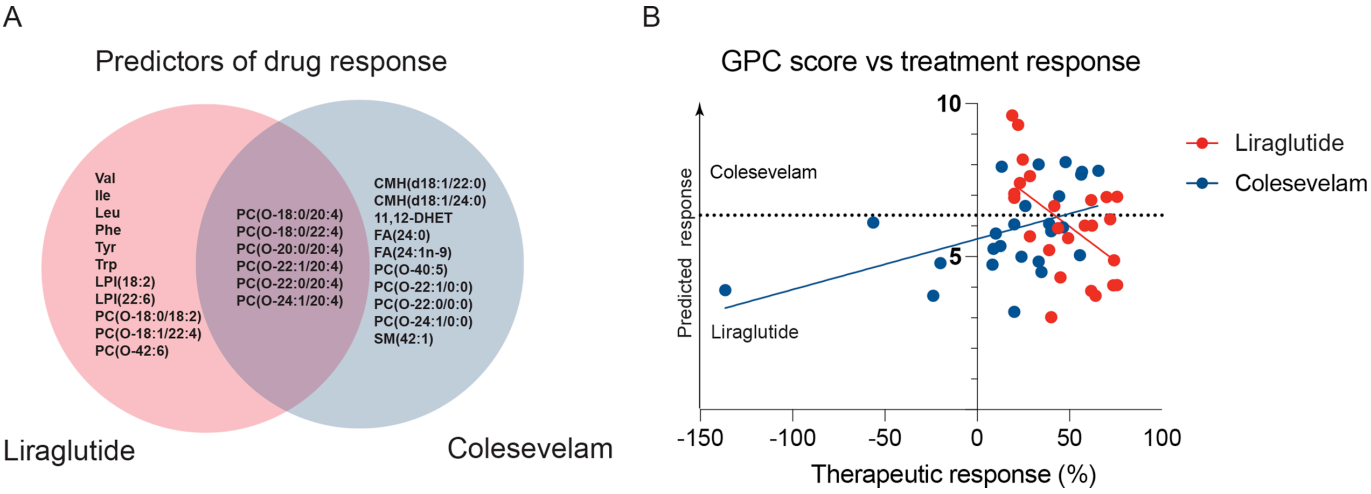

Figure 7 Glycerophosphocholines (GPCs) predict response to BAD treatment. (A) Venn diagram presenting number of metabolites predictive of response to treatment. (B) The linear relation between GPCs score and response to treatment expressed as % reduction on number of stools per week. Each dot represents one patient diagnosed with BAD, and the solid lines are trendlines (blue, colesevelam-treated patients; red, liraglutide-treated patients).

with cluster 2 (BAD_2). Importantly, we found no difference between the patients in these clusters in the baseline SeHCAT (%) or in the number of stools per day in a week (p=0.52 and p=0.28, respectively) (table 2). Next, we compared pairwise the two BAD clusters to the metabolomic profiles of patients with NAFLD (figure 6A,B, online supplemental table 5–6). In BAD_1 versus NAFLD, we identified 75 upregulated and 55 downregulated metabolites, whereas patients with BAD_2 only were defined by eight upregulated metabolites. This suggests that patients with BAD_2 are more alike to NAFLD, than BAD_1. Surprisingly, TGs were among the most upregulated metabolites in BAD_1, suggesting prominent dyslipidaemia. A previous study has linked hypertriglyceridaemia with FGF19 levels in patients with BAD[34]; however, FGF19 levels did not differ between BAD clusters (table 2) nor did it correlate with TG levels (p=0.185 in BAD_1, p=0.569 in BAD_2, p=0.988 in combined clusters). Furthermore, many of the downregulated metabolites were shared between the two BAD clusters (figure 6C), with significant depletion compared with CTRLs of unsaturated fatty acids, taurine, hypotaurine and phosphatidylcholines (online supplemental table 7).

Serum metabolomics predicts response to novel BAD treatment

Serum samples were collected from treatment-naive SeHCAT-verified patients with BAD enrolled into a phase 1b clinical trial (EudraCT 2018-003575-34) comparing the efficacy and safety of the GLP-1 receptor agonist liraglutide and the bile acid sequestrant colesevelam for the treatment of BAD.[19] We investigated if any metabolites before treatment correlated with the observed therapeutic response (% reduction in the number of stools/day) to the administered treatment.[19] We identified 17 metabolites that significantly correlated with the response to liraglutide (online supplemental table 8), and 16 metabolites were shown to correlate with the response to colesevelam (online supplemental table 9). Interestingly, six glycerophosphocholines (GPCs) overlapped between the two subgroups (figure 7A), showing a significant collinearity (Spearman r: 0.58–0.96) (online supplemental figure 5), which allowed us to calculate a GPC score. This score is the sum of the six metabolites (figure 7B) that showed a negative correlation with liraglutide ($Y=-0.04536 \times X + 8.251$, $R^2=0.3$, p=0.0045) and a positive correlation with colesevelam response ($Y=0.01653 \times X + 5.577$, $R^2=0.2412$, p=0.0127). Therefore, a higher GPC score and elevated metabolite concentrations are associated with an improved outcome on colesevelam. Importantly, and in line with the recent outcome of the clinical trial, a lower GPC score is predictive of a significant improvement of the BAD condition for patients treated with liraglutide. The GLP-1 receptor, which is the target of liraglutide, is a member of the G protein-coupled receptor family known to interfere with GPCs and thus, a higher GPC score could warrant a dose-adjustment of liraglutide.

DISCUSSION

In this study, we used comprehensive state-of-the-art metabolomics to investigate more than 1200 metabolites to distinguish patients with BAD from healthy individuals and patients suffering from NAFLD. We present the first comprehensive serum metabolome of patients with BAD, from which we developed a diagnostic model based on the concentrations of five metabolites with high predictive accuracy, that is, with an AUROC of 0.94 and 0.91 in the discovery and validation cohorts, respectively. Furthermore, we show that the model is independent of obesity and can distinguish patients with BAD from obese patients with NAFLD.

To succeed in developing a new diagnostic method, the new tool needs to supersede the existing methods in one or more ways. Comparing the BDS to SeHCAT,[35–37] both the sensitivity (70–100% for SeHCAT vs 78% for BDS) and the specificity (80–90% for SeHCAT vs 93% for BDS) were similar. Moreover, the BDS is less time-consuming and does not include radioactive exposure. Whether it would be cheaper is hard to say at this point since the price for a test with BDS in the clinic is unknown. However, this study warrants the development of an easy and cheap BDS assay to be used in the clinic, since using UHPLC-MS is not convenient or possible for routine clinical measurements.

Compared with measurements of serum C4 or FGF19, the BDS was superior in identifying true positives in our data set when using the standard cut-off value for C4 (>48.7 ng/mL) and for FGF19 (<145 pg/mL) (56% vs 70% vs 90%, respectively). As biomarkers, C4 and FGF19 do not seem to have clinical potential to stand alone due to low sensitivity, at least in our data set.

The reported sensitivity and specificity for serum C4 measurements vary greatly depending on population and cut-off values,[38] hence, making direct comparisons difficult. Furthermore, both C4 and FGF19 have diurnal variations,[39] thus, requiring sampling in the morning before 09:00, which is not relevant for the BDS. Overall, it seems that the BDS is superior to serum C4 and FGF19 measurements, but a prospective study with direct comparison is needed to properly compare the methods.

The machine learning approach used to identify the optimal number of metabolites in the present model and its components has previously been shown successful in the early detection of liver cancer and other diseases.[31] Using the combination of several metabolites, the simultaneous analysis of the metabolome can provide useful information not only for biomarker discovery, but also inform on biological relevance. Hence, the use of a data-driven, unbiased approach has revealed that the combination of the five specific metabolites of the BDS is consistently deregulated in patients with BAD. This might be a clue to unknown metabolic changes important in BAD pathophysiology. As such, decanoylcarnitine has been previously linked to an altered microbiome[40] and, thus, could associate with previously reported alterations in the BAD microbiome.[5] Future studies are needed to identify the possible link between these metabolites and BAD. Indeed, many circulating lipids are highly correlated with hepatic lipids,[41] which can reflect the alterations in the hepatic metabolic function. Furthermore, the present comprehensive metabolomic landscape of BAD shows increased levels of primary unconjugated and glycine-conjugated bile acids in systemic circulation. As such, bile acids act as signalling molecules[42] and metabolic integrators that activate nuclear farnesoid X receptor (FXR), which induces ceramide synthesis and increases serum and liver ceramide concentrations, orchestrates TG homoeostasis[43] and decreases release of GLP-1.[44] Thus, the present findings showing deregulated metabolites including upregulation of serum ceramides and TGs in patients with BAD may allude to novel pathophysiological processes in BAD (figure 4A). Indeed, previous studies have linked hypertriglyceridaemia to BAD[34 45] and correlated this with FGF19 levels. However, we did not observe a correlation of these features in our study. Furthermore, in patients with a total TG level within the normal range (<2 mmol/L), we detected significant alterations of specific TG profiles, linking bile acid-FXR-TG metabolism to patients with BAD.[46] Moreover, we demonstrated that the concentrations of six GPCs correlate with the response to BAD treatment, which perhaps in the future can be used to guide treatment selection.

The strength of this study is the well-defined patient with BAD cohort (SeHCAT-verified with retention <10%), feature-matched control donors and the reproducible design of the study. However, the relatively small sample size including a total of 50 patients diagnosed with BAD is a limitation and requires further, prospective validation. Furthermore, the study lacks a group of SeHCAT-referred, SeHCAT-negative patients. Whether the BDS can distinguish SeHCAT-negative from SeHCAT-positive patients needs to be investigated. Association of deregulated metabolites in BAD with the treatment response should be seen as preliminary data and should be tested in future clinical studies.

CONCLUSIONS

The serum metabolome is significantly altered in patients suffering from BAD. We were able to exploit these alterations to develop a highly accurate diagnostic model yielding a BDS from a single blood sample. We hope that this will form the basis for developing an easy, convenient and reliable blood test-based diagnostic method that can be used in primary care and ultimately decrease diagnostic delay. Such a test would likely increase chances of timely and relevant treatment and, thus, improve the lives of people suffering from BAD and decrease healthcare expenses. Furthermore, the serum lipidome can potentially predict treatment response, which opens the possibility of personalised treatments.

Author affiliations
[1]Health and Medical Sciences, University of Copenhagen Biotech Research and Innovation Centre, Copenhagen, Denmark
[2]Center for Clinical Metabolic Research, Copenhagen University Hospital - Herlev and Gentofte, Hellerup, Denmark
[3]Unit for The Clinical Management of Digestive Diseases and CIBERehd, Hospital Universitario de Valme, Sevilla, Spain
[4]HEVEPHARM, Physiology and Pharmacology, IBSAL, CIBERehd, University of Salamanca, Salamanca, Spain
[5]Steno Diabetes Center Copenhagen, Herlev, Denmark
[6]Department of Clinical Medicine, Faculty of Health and Medical Sciences, University of Copenhagen, Copenhagen, Denmark

Twitter Manuel Romero-Gómez @mromerogomez, Rocio I R Macias @rirmacias, Jesper B Andersen @jaboeje and Filip Krag Knop @Filip_Knop

Acknowledgements The authors are thankful to all study participants and acknowledge the administrative assistance from Research Secretary Anne-Grete L. Teisner and the experimental and laboratory assistance from lab-technicians Dorthe B. Nielsen and Kirsten H. Rasmussen from the Center for Clinical Metabolic Research, Copenhagen University Hospital – Herlev and Gentofte.

Contributors Study concept and design: ML, MLK, JBA, FKK. Data collection: ML, MLK. Analysis and interpretations of data: ML, MLK, A-MGE, JBA, FKK. Drafting the manuscript: ML, MLK, A-MGE, JBA, FKK. Revision of the manuscript: ML, MLK, A-MGE, MR-G, RIRM, JBA, FKK. Funding: ML, MLK, A-MGE, JBA, FKK. ML and MLK contributed equally to this paper; and JBA and FKK contributed equally to this paper. JBA and FKK are the gurantors of the present work.

Funding This project was supported by competitive funding from Læge Sofus Carl Emil Friis og Hustru Doris Friis' foundation. The laboratory of JBA is supported by the Novo Nordisk Foundation (14040, 0058419), Danish Cancer Society (R98-A6446, R167-A10784, R278-A16638) and the Danish Medical Research Council (4183-00118A, 1030-00070B).

Competing interests None declared.

Patient and public involvement Patients and/or the public were not involved in the design, or conduct, or reporting, or dissemination plans of this research.

Patient consent for publication Not applicable.

Ethics approval This study involves human participants and was approved by Danish Regional Ethics Committee approval (H-18048247). Participants gave informed consent to participate in the study before taking part.

Provenance and peer review Not commissioned; externally peer reviewed.

Data availability statement Data are available upon reasonable request.

ORCID iDs
Monika Lewinska http://orcid.org/0000-0002-5275-992X
Anne-Marie Gade Ellegaard http://orcid.org/0000-0002-4389-3908
Manuel Romero-Gómez http://orcid.org/0000-0001-8494-8947
Rocio I R Macias http://orcid.org/0000-0002-4748-0326

Jesper B Andersen http://orcid.org/0000-0003-1760-5244
Filip Krag Knop http://orcid.org/0000-0002-2495-5034

REFERENCES

1 Wilcox C, Turner J, Green J. Systematic review: the management of chronic diarrhoea due to bile acid malabsorption. *Aliment Pharmacol Ther* 2014;39:923–39.
2 Ao M, Sarathy J, Domingue J, *et al*. Chenodeoxycholic acid stimulates Cl (-) secretion via cAMP signaling and increases cystic fibrosis transmembrane conductance regulator phosphorylation in T84 cells. *Am J Physiol Cell Physiol* 2013;305:C447–56.
3 Bampton PA, Dinning PG, Kennedy ML, *et al*. The proximal colonic motor response to rectal mechanical and chemical stimulation. *Am J Physiol Gastrointest Liver Physiol* 2002;282:G443–9.
4 Camilleri M, Nurko S. Bile acid diarrhea in adults and adolescents. *Neurogastroenterol Motil* 2022;34:e14287.
5 Kårhus ML, Sonne DP, Thomasen M, *et al*. Enterohepatic, gluco-metabolic, and gut microbial characterization of individuals with bile acid malabsorption. *Gastro Hep Advances* 2022;1:299–312.
6 Vijayvargiya P, Camilleri M. Update on bile acid malabsorption: finally ready for prime time? *Curr Gastroenterol Rep* 2018;20:10.
7 Camilleri M. Advances in understanding of bile acid diarrhea. *Expert Rev Gastroenterol Hepatol* 2014;8:49–61.
8 Walters JRF. Defining primary bile acid diarrhea: making the diagnosis and recognizing the disorder. *Expert Rev Gastroenterol Hepatol* 2010;4:561–7.
9 Wedlake L, A'Hern R, Russell D, *et al*. Systematic review: the prevalence of idiopathic bile acid malabsorption as diagnosed by sehcat scanning in patients with diarrhoea-predominant irritable bowel syndrome. *Aliment Pharmacol Ther* 2009;30:707–17.
10 Farrugia A, Attard JA, Hanmer S, *et al*. Rates of bile acid diarrhoea after cholecystectomy: a multicentre audit. *World J Surg* 2021;45:2447–53.
11 Ruiz-Campos L, Gisbert JP, Ysamat M, *et al*. Systematic review with meta-analysis: the prevalence of bile acid malabsorption and response to colestyramine in patients with chronic watery diarrhoea and previous cholecystectomy. *Aliment Pharmacol Ther* 2019;49:242–50.
12 Sciarretta G, Furno A, Mazzoni M, *et al*. Post-cholecystectomy diarrhea: evidence of bile acid malabsorption assessed by sehcat test. *Am J Gastroenterol* 1992;87:1852–4.
13 Damsgaard B, Dalby HR, Krogh K, *et al*. Long-term effect of medical treatment of diarrhoea in 377 patients with sehcat scan diagnosed bile acid malabsorption from 2003 to 2016; a retrospective study. *Aliment Pharmacol Ther* 2018;47:951–7.
14 Andrae DA, Patrick DL, Drossman DA, *et al*. Evaluation of the Irritable Bowel Syndrome Quality of Life (IBS-QOL) questionnaire in diarrheal-predominant irritable bowel syndrome patients. *Health Qual Life Outcomes* 2013;11:208.
15 Paré P, Gray J, Lam S, *et al*. Health-related quality of life, work productivity, and health care resource utilization of subjects with irritable bowel syndrome: baseline results from LOGIC (longitudinal outcomes study of gastrointestinal symptoms in canada), a naturalistic study. *Clin Ther* 2006;28:1726–35.
16 Vijayvargiya P, Camilleri M, Carlson P, *et al*. Effects of colesevelam on bowel symptoms, biomarkers, and colonic mucosal gene expression in patients with bile acid diarrhea in a randomized trial. *Clin Gastroenterol Hepatol* 2020;18:2962–70.
17 Odunsi-Shiyanbade ST, Camilleri M, McKinzie S, *et al*. Effects of chenodeoxycholate and a bile acid sequestrant, colesevelam, on intestinal transit and bowel function. *Clin Gastroenterol Hepatol* 2010;8:159–65.
18 Orekoya O, McLaughlin J, Leitao E, *et al*. Quantifying bile acid malabsorption helps predict response and tailor sequestrant therapy. *Clin Med (Lond)* 2015;15:252–7.
19 Kårhus ML, Brønden A, Forman JL, *et al*. Safety and efficacy of liraglutide versus colesevelam for the treatment of bile acid diarrhoea: a randomised, double-blind, active-comparator, non-inferiority clinical trial. *Lancet Gastroenterol Hepatol* 2022;7:922–31.
20 Jellema P, van der Windt DAWM, Schellevis FG, *et al*. Systematic review: accuracy of symptom-based criteria for diagnosis of irritable bowel syndrome in primary care. *Aliment Pharmacol Ther* 2009;30:695–706.
21 Kurien M, Thurgar E, Davies A, *et al*. Challenging current views on bile acid diarrhoea and malabsorption. *Frontline Gastroenterol* 2018;9:92–7.
22 Poon D, Law GR, Major G, *et al*. A systematic review and meta-analysis on the prevalence of non-malignant, organic gastrointestinal disorders misdiagnosed as irritable bowel syndrome. *Sci Rep* 2022;12:1949.
23 Nyhlin H, Merrick MV, Eastwood MA, *et al*. Evaluation of ileal function using 23-selena-25-homotaurocholate, a-gamma-labeled conjugated bile acid. Initial clinical assessment. *Gastroenterology* 1983;84:63–8.
24 Vijayvargiya P, Camilleri M, Shin A, *et al*. Methods for diagnosis of bile acid malabsorption in clinical practice. *Clin Gastroenterol Hepatol* 2013;11:1232–9.
25 Fromm H, Hofmann AF. Breath test for altered bile-acid metabolism. *Lancet* 1971;2:621–5.
26 Scarpello JH, Sladen GE. Appraisal of the 14C-glycocholate acid test with special reference to the measurement of faecal 14C excretion. *Gut* 1977;18:742–8.
27 Borup C, Wildt S, Rumessen J, *et al*. Biochemical diagnosis of bile acid diarrhea: prospective comparison with the 75seleno-taurohomocholic acid test. *Am J Gastroenterol* 2020;115:2086–94.
28 Vijayvargiya P, Camilleri M, Carlson P, *et al*. Performance characteristics of serum C4 and FGF19 measurements to exclude the diagnosis of bile acid diarrhoea in IBS-diarrhoea and functional diarrhoea. *Aliment Pharmacol Ther* 2017;46:581–8.
29 Vijayvargiya P, Camilleri M, Taylor A, *et al*. Combined fasting serum C4 and primary bile acids from a single stool sample to diagnose bile acid diarrhea. *Gastroenterology* 2020;159:1952–4.
30 Pattni SS, Brydon WG, Dew T, *et al*. Fibroblast growth factor 19 in patients with bile acid diarrhoea: a prospective comparison of FGF19 serum assay and sehcat retention. *Aliment Pharmacol Ther* 2013;38:967–76.
31 Lewinska M, Santos-Laso A, Arretxe E, *et al*. The altered serum lipidome and its diagnostic potential for non-alcoholic fatty liver (NAFL)-associated hepatocellular carcinoma. *EBioMedicine* 2021;73:103661.
32 Pang Z, Chong J, Zhou G, *et al*. MetaboAnalyst 5.0: narrowing the gap between RAW spectra and functional insights. *Nucleic Acids Res* 2021;49:W388–96.
33 Gaud C, C Sousa B, Nguyen A, *et al*. BioPAN: a web-based tool to explore mammalian lipidome metabolic pathways on lipid maps. *F1000Res* 2021;10:4.
34 Johnston IM, Nolan JD, Pattni SS, *et al*. Characterizing factors associated with differences in FGF19 blood levels and synthesis in patients with primary bile acid diarrhea. *Am J Gastroenterol* 2016;111:423–32.
35 Notghi A, O'Brien J, Low CS, *et al*. Measuring sehcat retention: a technical note. *Nucl Med Commun* 2011;32:960–6.
36 Sciarretta G, Vicini G, Fagioli G, *et al*. Use of 23-selena-25-homocholyltaurine to detect bile acid malabsorption in patients with illeal dysfunction or diarrhea. *Gastroenterology* 1986;91:1–9.
37 Baena García A, Partida Palma F, García Martínez S, *et al*. 75Se-homocholic acid taurine scintigraphy (75sehcat®), a standard benchmark test in bile acid malabsorption? *Rev Esp Med Nucl Imagen Mol (Engl Ed)* 2019;38:305–11.
38 Lyutakov I, Ursini F, Penchev P, *et al*. Methods for diagnosing bile acid malabsorption: a systematic review. *BMC Gastroenterol* 2019;19:185.
39 Brydon WG, Culbert P, Kingstone K, *et al*. An evaluation of the use of serum 7-alpha-hydroxycholestenone as a diagnostic test of bile acid malabsorption causing watery diarrhea. *Can J Gastroenterol* 2011;25:319–23.
40 Chen L, Wang S, Zhang Y, *et al*. Multi-omics reveals specific host metabolism-microbiome associations in intracerebral hemorrhage. *Front Cell Infect Microbiol* 2022;12:999627.
41 Ooi GJ, Meikle PJ, Huynh K, *et al*. Hepatic lipidomic remodeling in severe obesity manifests with steatosis and does not evolve with non-alcoholic steatohepatitis. *J Hepatol* 2021;75:524–35.
42 Chiang JYL. Bile acid metabolism and signaling. *Compr Physiol* 2013;3:1191–212.
43 Jiao Y, Lu Y, Li X. Farnesoid X receptor: a master regulator of hepatic triglyceride and glucose homeostasis. *Acta Pharmacol Sin* 2015;36:44–50.
44 Trabelsi M-S, Daoudi M, Prawitt J, *et al*. Farnesoid X receptor inhibits glucagon-like peptide-1 production by enteroendocrine L cells. *Nat Commun* 2015;6:7629.
45 Angelin B, Hershon KS, Brunzell JD. Bile acid metabolism in hereditary forms of hypertriglyceridemia: evidence for an increased synthesis rate in monogenic familial hypertriglyceridemia. *Proc Natl Acad Sci U S A* 1987;84:5434–8.
46 Sagar NM, McFarlane M, Nwokolo C, *et al*. Mechanisms of triglyceride metabolism in patients with bile acid diarrhea. *World J Gastroenterol* 2016;22:6757–63.